

Experimental determination technique for magnetic anisotropy of individual nanowires

Kyoung-Woong Moon^a, Jae-Chul Lee^{a,b}, Sug-Bong Choe^{a*}, Kyung-Ho Shin^b

^aCenter for Subwavelength Optics and School of Physic and Astronomy, Seoul National University, Seoul 151-742, Republic of Korea

^bSpintronics Research Center, Korea Institute of Science and Technology, Seoul 136-791, Republic of Korea

ARTICLE INFO

Article history:

Received 15 December 2008

Received in revised form 16 February 2009

Accepted 19 February 2009

Available online 6 March 2009

PACS:

75.30.Gw

75.75.+a

Keywords:

Magnetic anisotropy

Ferromagnetic nanowires

Torque magnetometer

Anisotropic magnetoresistance

ABSTRACT

We present an experimental technique to determine the magnetic anisotropy of ferromagnetic nanowires. In the technique, the magnetization state is monitored by measuring the anisotropic magnetoresistance with rotating the external magnetic field. The measured magnetoresistance curves exhibit basically the same curves typically appeared in the torque magnetometric measurements, which are then readily analyzed based on the Stoner–Wohlfarth theory with a single fitting parameter – the magnetic anisotropy. By applying the present technique to Permalloy nanowires, it is shown that the shape anisotropy in real nanowires is significantly influenced by the edge roughness.

© 2009 Elsevier B.V. All rights reserved.

Recently, a number of versatile nanodevices have been proposed based on the ferromagnetic nanostructures [1–4]. Such devices are operated by manipulating the magnetization state of the nanostructures either by applying the magnetic field or by injecting the electric current. To accomplish the device operation, it is crucial to quantify the magnetic properties such as the saturation magnetization and the magnetic anisotropy, since the magnetic configuration and the dynamic process are governed by them [5,6]. There have been developed the conventional magnetometers such as the vibrating sample magnetometer (VSM) [7], the superconducting quantum interference devices (SQUID) [8], the torque magnetometer [9], etc. to measure the magnetic properties. However, they are designed for bulk and/or film diagnosis and thus, direct probe onto individual nanostructures is not readily applicable due to the weak signal from small volume of the nanostructures.

In this letter, we present a magnetometric technique to measure the magnetic anisotropy of ferromagnetic nanowires. The technique basically utilizes the typical analysis methods originally developed for the torque magnetometer, but instead of measuring the torque curves, the anisotropic magnetoresistance (AMR) is measured with rotating the external magnetic field. The magnetic anisotropy is then determined by fitting the AMR curves based on

the Stoner–Wohlfarth theory [10]. The technique is applied to Permalloy nanowires to confirm the validity of the technique in comparison with the analytic predictions.

Fig. 1a illustrates the schematic setup of the AMR measurement. By applying an external magnetic field H with an angle φ to the nanowire length axis, the magnetization M rotates to an angle θ for the energy minimum between the Zeeman energy and the anisotropy energy. When the current flows through the nanowires, the non-collinear magnetization with respect to the current induces the change in the electric resistance – namely the AMR effect [11], which is given by $R(\theta) = R(0) - \Delta R \sin^2 \theta$, where ΔR is the maximum resistance change. The resistance measurement is carried out by measuring the voltage drop through the nanowire under a constant electric current (typically 100 μA) in the typical two-probe scheme as shown in Fig. 1b. The accuracy of the resistance measurement is 10^{-5} relative to the total resistance.

The nanowire structures with different widths ranging from 130 to 820 nm were patterned onto 20-nm-thick Permalloy films. All the nanowires were 17 μm long with tapered ends as shown by the secondary electron microscopy (SEM) image in Fig. 1b. For the sample preparation, 4 nm Ta/20 nm $\text{Ni}_{80}\text{Fe}_{20}$ /4 nm Ta films were first deposited onto Si wafer by dc-magnetron sputtering under 2 mTorr Ar pressure with 1×10^{-8} T base pressure at the ambient temperature. The saturation magnetization M_S of the films was measured to be 1.1 T by an alternating gradient magnetometer. The nanowires were then patterned by e-beam lithography onto

* Corresponding author. Tel.: +82 2 880 9254; fax: +82 2 884 3002.

E-mail address: sugbong@snu.ac.kr (S.-B. Choe).

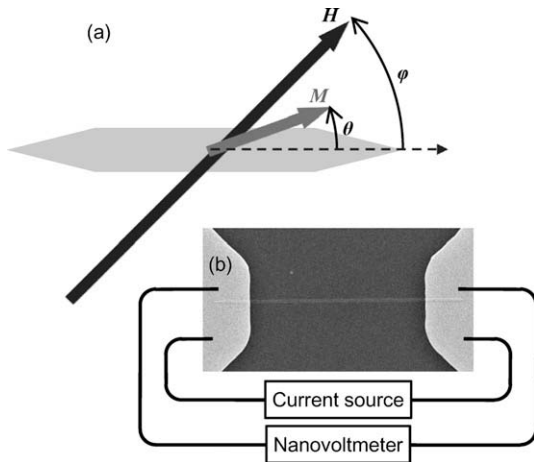


Fig. 1. (a) Schematic drawing of the angles of the applied field H and the magnetization M with respect to the nanowire axis. (b) Setup for the AMR measurement with a current source and a nanovoltmeter. The image shows the nanowire structure captured by a SEM.

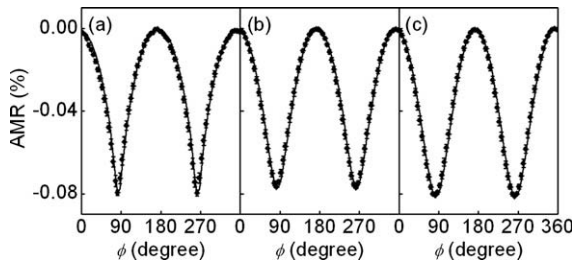


Fig. 2. The resistance (circular symbols) measured from the 230-nm-wide nanowire with rotating ϕ of the external magnetic field, (a) 100 mT, (b) 200 mT, and (c) 300 mT, respectively. The best fit (solid lines) by the Stoner-Wohlfarth theory.

the spin-coated e-beam resist (maN-2403), followed by the ion milling. Finally, 100 nm-thick Cu electrodes for the resistance measurement were deposited by the lift-off process with optical lithography.

The typical AMR curves with respect to the rotating angle ϕ of an external magnetic field are plotted in Fig. 2. The circular dots in the figure are the resistance measured from the 230-nm-wide nanowire under the strengths of the external magnetic field, (a) 100 mT, (b) 200 mT, and (c) 300 mT, respectively. For the case when the applied magnetic field is sufficiently large as discussed later, one can extract the magnetization state by normalizing the AMR curves as $\sin^2 \theta = [R(0) - R(\theta)]/\Delta R$. It is then directly compared with the Stoner-Wohlfarth theory [10]. In the theory, the magnetic energy E is composed of the anisotropy energy and the Zeeman energy as given by $E = -K \cos^2 \theta - M_s H \cos(\theta - \phi)$, where K is the uniaxial magnetic anisotropy constant. The dimensionless form of the energy equation is then rewritten to be $e = E/K = -\cos^2 \theta - 2(H/H_K) \cos(\theta - \phi)$ with the anisotropy field H_K defined as $H_K \equiv 2K/M_s$. At equilibrium, θ is determined by the energy minimization condition, $\frac{\partial e}{\partial \theta} = \sin 2\theta + 2(H/H_K) \sin(\theta - \phi) = 0$. The solution of the equation has been analytically derived in a closed-form in Ref. [12]. The solid lines in Fig. 2 exhibit the best fit with the solution of the equation. The absolute coincidence with the experimental data confirms the validity of this approach.

The anisotropy field H_K , determined by the best fit, is plotted with respect to H in Fig. 3 for the nanowires with the widths, (a) 130 nm, (b) 230 nm, (c) 330 nm, (d) 410 nm, (e) 530 nm, and (f) 610 nm, respectively. All the figures clearly show that a constant H_K is determined for H larger than a threshold. The threshold is

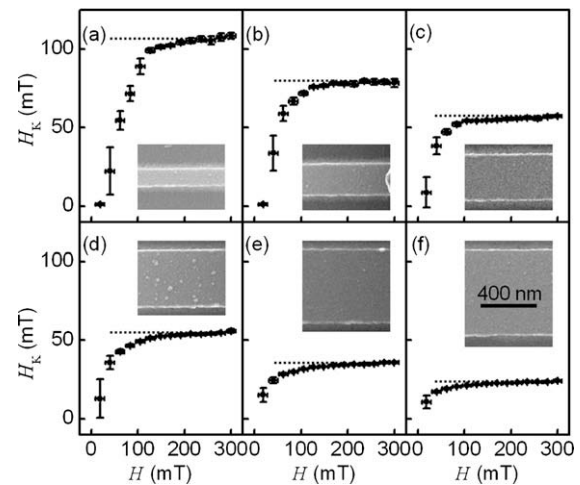


Fig. 3. The anisotropy field H_K with respect to the applied field H for the nanowires with the widths of (a) 130 nm, (b) 230 nm, (c) 330 nm, (d) 410 nm, (e) 530 nm, and (f) 610 nm, respectively. The saturation value of H_K (dot lines). The inset shows the SEM images at the scale for each nanowire.

predicted to be equal to H_K from the Stoner-Wohlfarth theory. Below the threshold, the present analysis technique fails due to the ambiguity in determination of ΔR , since the magnetization does not reverse (or reverses abruptly) under an insufficient magnetic field strength. However, above the threshold, the magnetization rotates gradually across the wire width axis and thus, the resistance changes in the full ΔR scale. In this regime, the AMR curves exhibit four-fold symmetry as seen in Fig. 2. One can therefore easily check the sufficiency of the applied field strength from the profiles of the AMR curves. In practice, it is wise to measure the AMR curve under the maximum field strength of the electromagnet, since a constant H_K is determined above the threshold.

Fig. 4 summarizes the results for the nanowires with different widths. The circular dots indicate the averaged values for $H > 200$ mT for each nanowire. The left axis is scaled with the anisotropy field H_K and the right axis is scaled with the magnetic anisotropy constant K . The magnetic anisotropy is decreased with increasing the wire width, which is ascribed to the reduction of the shape anisotropy with reducing the aspect ratio of the length over the width of the nanowires.

It is worthwhile to note that the experimental values of H_K and K are significantly smaller than those of ideal nanowires. By consider-

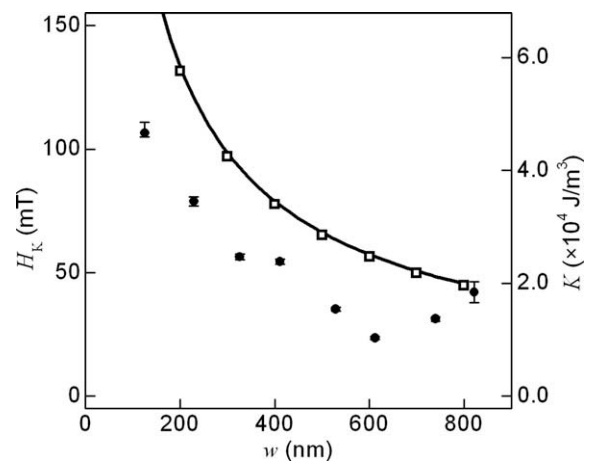


Fig. 4. The experimental values of H_K and K with respect to the wire width w (solid symbols). The analytic prediction for nanowires with ideal edges (solid line). And the simulation-based results for ideal nanowires (open symbols).

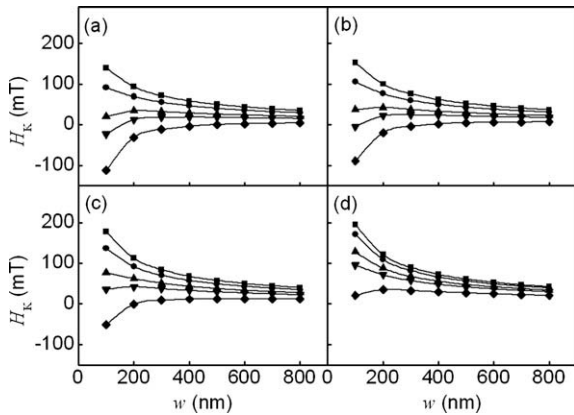


Fig. 5. The simulated values of H_K with respect to the wire width w for the sinusoidal edge roughness. The period of the roughness is (a) 10 nm, (b) 20 nm, (c) 40 nm, and (d) 80 nm, respectively. The amplitude of the roughness is 6 nm (square), 10 nm (circle), 16 nm (up triangle), 20 nm (down triangle), and 30 nm (diamond), respectively.

ing an infinitely long cuboid as an ideal nanowire, it is analytically given that the demagnetizing factor N_w along the width axis is [13]

$$N_w = \frac{2}{\pi} \tan^{-1} \left(\frac{w}{t} \right) - \frac{w}{2\pi t} \log \left[1 + \left(\frac{t}{w} \right)^2 \right] + \frac{t}{2\pi w} \log \left[1 + \left(\frac{w}{t} \right)^2 \right], \quad (1)$$

where t is the thickness of the nanowire. The demagnetizing factor along the length axis vanishes in this geometry. The shape anisotropy and the anisotropy field between the width and the length axes are therefore given by $K = N_w M_s^2 / 2$ and $H_K = N_w M_s$, respectively. The values are plotted by the solid line in Fig. 4. Significant discrepancy is seen between the ideal cuboids and the real nanowires. The discrepancy is possibly caused either by the structural imperfection such as the rough edges, non-planar interfaces, and irregular grains, or by the magnetic damage from patterning and oxidation at the wire edges, which are excluded in the ideal cuboids. The effect from the finite length and the tapered ends is also tested, but found to be negligible due to the long wire geometry.

To check whether the discrepancy is originated from our analysis technique, we generate the AMR curves by micromagnetic simulations and then, apply the analysis technique to determine H_K and K . The micromagnetic simulation is carried out by the object-oriented micromagnetic framework (oommf) [14] for the ideal cuboid geometry. The periodic boundary condition is adopted along the length axis [15], and 2 nm cubic cells are used. The open

square dots in Fig. 4 show the analysis results. The absolute conformity with the solid line of the analytic prediction verifies the validity of the present analysis technique. From this test, the accuracy of the technique is turned out to be better than 2%.

As a reference, the effect of the edge roughness is examined by micromagnetic calculation. For this case, we calculate the magnetostatic energy of the magnetization states saturated either along the width axis or along the length axis. The shape anisotropy is then obtained by the difference of the magnetostatic energy between the two states. Fig. 5 shows the values of H_K of the nanowires with sinusoidal edge roughness. As already discussed in the study of the orange-peel coupling [16,17], the edge roughness reduces significantly the shape anisotropy [18] and the results get closer to the experimental values. In some cases, intensely distorted edge with large roughness amplitude and small period shows the negative values of H_K . It means that the magnetization direction of the nanowire no more prefer the wire length direction.

Acknowledgements

This study was supported by the Korea Science and Engineering Foundation through the NRL program (ROA-2007-000-20032-0). KWM was supported by the Seoul R&BD program.

References

- [1] S.S.P. Parkin, M. Hayashi, L. Thomas, *Science* 320 (2008) 190.
- [2] D.A. Allwood, G. Xiong, C.C. Faulkner, D. Atkinson, D. Petit, R.P. Cowburn, *Science* 309 (2005) 688.
- [3] S.I. Kiselev, J.C. Sankey, I.N. Krivorotov, N.C. Emley, R.J. Schoelkopf, R.A. Buhrman, D.C. Ralph, *Nature* 425 (2003) 380.
- [4] A.A. Tulapurkar, Y. Suzuki, A. Fukushima, H. Kubota, H. Maehara, K. Tsunekawa, D.D. Djayaprawira, N. Watanabe, S. Yuasa, *Nature* 438 (2005) 339.
- [5] S.-B. Choe, S.-C. Shin, *Appl. Phys. Lett.* 80 (2002) 1791.
- [6] S.-W. Jung, W. Kim, T.-D. Lee, K.-J. Lee, H.-W. Lee, *Appl. Phys. Lett.* 92 (2008) 202508.
- [7] E.O. Samwel, T. Bolhuis, J.C. Lodder, *Rev. Sci. Inst.* 69 (1998) 3204.
- [8] K. Takeda, H. Mori, A. Yamaguchi, H. Ishimoto, T. Nakamura, S. Kuriki, T. Hozumi, S.-I. Ohkoshi, *Rev. Sci. Inst.* 79 (2008) 033909.
- [9] A.K. Agarwala, *Rev. Sci. Inst.* 59 (1988) 2265.
- [10] E.C. Stoner, E.P. Wohlfarth, *IEEE Trans. Magn.* 27 (1991) 3475.
- [11] I.A. Campbell, A. Fert, *Transport Properties of Ferromagnets*, in *Ferromagnetic Materials*, vol. 3, North-Holland, Amsterdam, 1982, p. 747.
- [12] J. Hur, M.C. Paek, K.-I. Cho, S.-C. Shin, *Appl. Phys. Lett.* 76 (2000) 472.
- [13] S.-B. Choe, *Appl. Phys. Lett.* 92 (2008) 062506.
- [14] M. Donahue, D. Porter, (2000, October 30). OOMMF (1.2a4 ver.) [Online]. Available: <<http://math.nist.gov/oommf/>>.
- [15] K. Lebecki, (2006, December 1). OOMMF_PBC (1.2a4 ver.) [Online]. Available: <<http://info.ifpan.edu.pl/~lebecki/pbc.htm/>>.
- [16] P. Bruno, *J. Appl. Phys.* 64 (1988) 3153.
- [17] L. Néel, *Comptes Rendus Acad. Sci.* 255 (1962) 1676.
- [18] S.-B. Choe, S.-C. Shin, *J. Magn. Magn. Mater.* 221 (2000) 255.